Simultaneous Monitoring of Changes in Magnesium and Calcium Concentrations in Frog Cut Twitch Fibers Containing Antipyrylazo III

MALCOLM IRVING, JAMES MAYLIE, NING LEUNG SIZTO, and W. KNOX CHANDLER

From the Department of Calcium and Magnesium Physiology, Yale University School of Medicine, New Haven, Connecticut 06510

ABSTRACT Antipyrylazo III was introduced into frog cut twitch fibers (17–19°C) by diffusion. After action potential stimulation, the change in indicator absorbance could be resolved into two components that had different time courses and wavelength dependences. The first component was early and transient and due to an increase in myoplasmic free [Ca] (Maylie, J., M. Irving, N.L. Sizto, and W.K. Chandler, 1987, *Journal of General Physiology*, 89:83–143). The second component, usually measured at 590 nm (near the isosbestic wavelength for Ca), developed later than the Ca transient and returned towards baseline about 100 times more slowly. Although the wavelength dependence of this component is consistent with an increase in either free [Mg] or pH, its time course is clearly different from that of the signals obtained with the pH indicators phenol red and 4',5'-dimethyl-5-(and -6-) carboxyfluorescein, suggesting that it is mainly due to an increase in free [Mg]. After a single action potential in freshly prepared cut fibers that contained 0.3 mM antipyrylazo III, the mean peak amplitude of $\Delta A(590)$ would correspond to an increase in free [Mg] of 47 μM if all the signal were due to a change in [Mg] and all the intracellular indicator reacted with Mg as in cuvette calibrations. With either repetitive action potential stimulation or voltage-clamp depolarization, the $\Delta A(590)$ signal continued to develop throughout the period when free [Ca] was elevated and then recovered to within 40–90% of the prestimulus baseline with an average rate constant between 0.5 and 1.0 s^{-1}. With prolonged voltage-clamp depolarization, both the amplitude and rate of development of the $\Delta A(590)$ signal increased with the amplitude of the depolarization and appeared to saturate at levels corresponding to an increase in free [Mg] of 0.8–1.4 mM and a maximum rate constant of 3–4 s^{-1}, respectively. These results are consistent with the idea

Address reprint requests to Dr. W. Knox Chandler, Department of Physiology, Yale University School of Medicine, 333 Cedar Street, P.O. Box 3333, New Haven, CT 06510-8026.

Dr. Irving's present address is Department of Biophysics, Cell and Molecular Biology, King's College London, 26-29 Drury Lane, London WC2B 5RL, England; Dr. Maylie's is Department of Obstetrical Research, Oregon Health Sciences University, 3181 S.W. Sam Jackson Park Road, Portland, OR 97201; and Dr. Sizto's is 3154 Waugh Place, Fremont, CA 94536.

J. GEN. PHYSIOL. © The Rockefeller University Press · 0022-1295/89/04/0585/24 $2.00
Volume 93 April 1989 585–608

that the $\Delta A(590)$ signal is primarily due to changes in myoplasmic free [Mg] produced by a change in the Mg occupancy of the Ca,Mg sites on parvalbumin that results from the Ca transient.

INTRODUCTION

The experiments described in this paper were carried out on frog cut muscle fibers (Hille and Campbell, 1976) that contained antipyrylazo III, which was first used in muscle as a Ca indicator by Kovacs et al. (1979). The absorbance of this indicator, however, is sensitive to the level of pH and free [Mg], as well as free [Ca]. The absorbance change produced by a change in free [Ca] has a very different wavelength dependence from that produced by a change in either pH or free [Mg]. The Ca-dependent absorbance change is large at 720 nm and zero near 590 nm (the isosbestic wavelength), whereas both the pH- and Mg-dependent absorbance changes are large at 590–600 nm but almost zero at 720 nm (Baylor et al., 1982*b*, 1985, 1986). With measurements of antipyrylazo III-related absorbance at 720 and 590 nm, it is possible to monitor changes in both myoplasmic Ca and Mg/pH with one indicator. After action potential stimulation of intact fibers injected with antipyrylazo III, the Ca signal is early and brief whereas the Mg/pH signal develops later and recovers much more slowly (Baylor et al., 1982*b*, 1983*b*, 1985).

As far as we are aware, the Mg/pH signal had not been observed in cut fibers before we began this series of experiments, from which an analysis of Ca signals has already been published (Maylie et al., 1987*c*). Here we describe simultaneous measurements of Ca and Mg/pH signals resulting from single and multiple action potential stimulation and from voltage-clamp depolarization of cut fibers. These results confirm those obtained earlier from intact fibers studied with single action potential stimulation. They also provide new information about the time course of development of the Mg/pH signal during repetitive action-potential or voltage-clamp stimulation and of recovery of the signal after repolarization. This information may be helpful in understanding some of the events associated with the contraction-relaxation cycle.

As in intact fibers, the wavelength dependence of the slowly recovering component of the absorbance signal is similar, but not identical, to either the pH- or Mg-difference spectrum. It is therefore not possible to separate, on the basis of wavelength dependence alone, the individual contributions made by changes in pH and Mg. The time course of the Mg/pH signal, however, is very different from that of the pH change measured with either phenol red or 4′, 5′-dimethyl-5- (and -6-) carboxyfluorescein (Me_2CF). This difference makes it likely that the slowly recovering antipyrylazo III signal is mainly due to an increase in myoplasmic free [Mg]. Many properties of this signal are consistent with the idea that it is due to Mg dissociating from parvalbumin as a result of the increase in myoplasmic free [Ca].

A preliminary report of some of this work has been given (Maylie et al., 1985).

METHODS

Experiments were carried out on cut twitch muscle fibers (Hille and Campbell, 1976) from cold-adapted *Rana temporaria*. The fibers were mounted in a double Vaseline-gap chamber,

similar to that used by Kovacs et al. (1983). To facilitate indicator entry, the surface membranes in the end pools were made permeable by a 2-min exposure to 0.01% saponin (Endo and Iino, 1980). Optical measurements were made with a 50-μm diameter spot of light focused on the middle of the fiber in the central-pool region. The intensity of transmitted light was measured simultaneously at three different wavelengths and two planes of linear polarization with the apparatus described in Irving et al. (1987). Details concerning the experimental method and the processing of optical records are given in that paper and in Maylie et al. (1987*b*, *c*). The measurements of transmitted light intensities have been expressed in terms of indicator-related absorbance; the procedures described in Maylie et al. (1987*b*, *c*) were used to subtract contributions that arose from the intrinsic optical properties of fibers. With mode 1 recording (Irving et al., 1987), the absorbances have been given as a 1:2 average of (absorbance of light linearly polarized along the fiber axis, i.e., 0° light):(absorbance of light linearly polarized perpendicular to the fiber axis, i.e., 90° light). With mode 2 recording, 1:1 averages have been used. The sarcomere spacing was 3.7–4.1 μm, the resting membrane potential was −90 mV, and the temperature was usually 17–19°C.

Most of the experiments were carried out with antipyrylazo III (ICN K & K Laboratories, Plainview, NY). Properties of Ca signals from these fibers are described in Maylie et al. (1987*c*). According to Rios and Schneider (1981), antipyrylazo III forms predominantly 1:2 complexes of Ca:indicator and 1:1 complexes of Mg:indicator under the conditions of our experiments, with the Mg:indicator complex having a dissociation constant of 6.7 mM. Changes in pH or free [Mg] were estimated by multiplying the observed values of indicator-related $\Delta A(590)/A(550)$ by either −2.5 pH units for pH (from cuvette calibrations of Baylor et al., 1982*b*; based on free [Mg] = 2 mM) or −15 mM for Mg (Baylor et al., 1986; based on a pH of 6.90). The Mg calibration constant, obtained by subtracting the cuvette spectra in the absence of Mg from those in the presence of 1.61–1.91 mM free [Mg], is almost independent of antipyrylazo III concentration in the range 0.4–1.6 mM; it is −14.8 mM with 0.4 mM antipyrylazo III and −15.2 mM with 1.6 mM (Fig. 16, *C* and *D*, respectively, from Baylor et al., 1986). Therefore, the average value, −15 mM, was used to estimate changes in free [Mg] inside our cut fibers in which the value of resting free [Mg] is assumed to be equal to that in the internal solution, 1 mM (Table I of Irving et al., 1987).

To determine the time course of changes in myoplasmic pH after action potential stimulation, a few experiments were carried out in which one of the pH indicators, phenol red (Flow Laboratories, Inc., Rockville, MD) and 4′,5′-dimethyl-5- (and -6-) carboxyfluorescein (Me_2CF) (Molecular Probes, Inc., Eugene, OR), was added to the end-pool solutions. The myoplasmic concentration of indicator at the optical recording site was estimated from measurements of indicator-related absorbance at the isosbestic wavelength, λ_{iso}, and the corresponding value of the molar extinction coefficient obtained from cuvette calibrations. For phenol red, λ_{iso} = 480 nm and $\epsilon(480) = 1.1 \times 10^4\ M^{-1}cm^{-1}$ (Lisman and Strong, 1979); for Me_2CF, λ_{iso} = 470 nm and $\epsilon(470) = 1.9 \times 10^4\ M^{-1}cm^{-1}$ (Chaillet and Boron, 1985).

Near pH 7, phenol red and Me_2CF may exist in two states of protonation. The fraction of indicator in each state is determined by a single dissociation constant. These two states will be referred to as protonated and nonprotonated. The fraction, f, that is not protonated can be determined from measurements of absorbance,

$$f = \frac{A(\lambda)/A(\lambda_{iso}) - r_{min}(\lambda)}{r_{max}(\lambda) - r_{min}(\lambda)}. \quad (1)$$

λ is selected so that changes in pH give large changes in $A(\lambda)$; $r_{min}(\lambda)$ and $r_{max}(\lambda)$ are the limiting values of $A(\lambda)/A(\lambda_{iso})$ for fully protonated and nonprotonated indicator, respectively. If the pK of the indicator is known, the value of pH can be calculated from f with the well-

known relation:

$$\mathrm{pH} = \mathrm{pK} + \log\left(\frac{f}{1-f}\right). \tag{2}$$

Small changes in f and pH can be calculated from the differential forms of Eqs. 1 and 2. The equations for Δf, $\Delta f/f$, and ΔpH are

$$\Delta f = \frac{\Delta A(\lambda)/A(\lambda_{iso})}{r_{max}(\lambda) - r_{min}(\lambda)}, \tag{3}$$

$$\frac{\Delta f}{f} = \frac{\Delta A(\lambda)/A(\lambda_{iso})}{A(\lambda)/A(\lambda_{iso}) - r_{min}(\lambda)}, \tag{4}$$

and

$$\Delta\mathrm{pH} = \frac{1}{\ln(10)} \cdot \frac{1}{(1-f)} \cdot \frac{\Delta f}{f}. \tag{5}$$

Eqs. 1–5 can be applied to measurements of the absorbance of an indicator inside cells if the indicator molecules behave as a single population, with single values of pK, r_{min} (λ), and r_{max} (λ). Under these conditions, the values of f and Δf, and consequently of ΔpH, can be obtained from absorbance measurements without knowing the pK of the indicator; only the values of $r_{min}(\lambda)$ and $r_{max}(\lambda)$ are needed. The value of the pK is used only to estimate resting pH, Eq. 2.

With phenol red, the absorbance at 570 nm was used to monitor changes in pH and a value of 7.7 was used for the pK (Lisman and Strong, 1979; Baylor and Hollingworth, personal communication); $r_{min}(570) \sim 0$ and $r_{max}(570) = 3.6$ (estimated from the calibrations of Baylor et al., 1982*a*, to apply to measurements made with our filters). Since $r_{min}(\lambda) \sim 0$, Eq. 4 reduces to $\Delta f/f \sim \Delta A(\lambda)/A(\lambda)$ and Eq. 5 can be replaced with

$$\Delta\mathrm{pH} \sim \frac{1}{\ln(10)} \cdot \frac{1}{(1-f)} \cdot \frac{\Delta A(\lambda)}{A(\lambda)}. \tag{6}$$

With Me_2CF, the absorbance at 510 nm was used to monitor changes in pH. According to Chaillet and Boron (1985), pK = 6.96, $r_{min}(510) = 0.71$, and $r_{max}(510) = 2.83$.

RESULTS

Wavelength Dependence of the Slowly Recovering Antipyrylazo III Signal

Fig. 1 *A* shows antipyrylazo III-related absorbance changes at six different wavelengths after single action potential stimulation. The signals show an early transient absorbance change, seen most clearly in the 520-, 550-, and 720-nm traces. The wavelength dependence of this component matches the Ca-difference spectrum (Maylie et al., 1987*c*). A second component of the antipyrylazo III absorbance change, seen most clearly in the 590- and 600-nm traces, does not recover towards baseline in the recording period shown in Fig. 1 *A* and has a very different wavelength dependence. These traces are similar to those obtained from intact fibers (Baylor et al., 1982*b*, 1985).

The amplitude of the slowly recovering component of the change in antipyrylazo III absorbance was measured 200–300 ms after stimulation, when the Ca signal had returned to baseline, and this amplitude is plotted against wavelength in Fig. 1 *B*

(circles). The continuous curve is the cuvette Mg-difference spectrum from Fig. 16 *C* in Baylor et al. (1986), scaled to match the fiber absorbance change at 600 nm. The curve provides a good fit to the fiber data between 550 and 650 nm but shows deviations at $\lambda \leqq 520$ nm and $670 \leqq \lambda \leqq 720$ nm. The cuvette pH-difference spectrum is similar to the Mg-difference spectrum (Baylor et al., 1982*b*) and also provides an approximate fit to the fiber data (not shown). Hence, the wavelength dependence of the slowly recovering antipyrylazo III signal is consistent with its being due to an increase in either free [Mg] or pH.

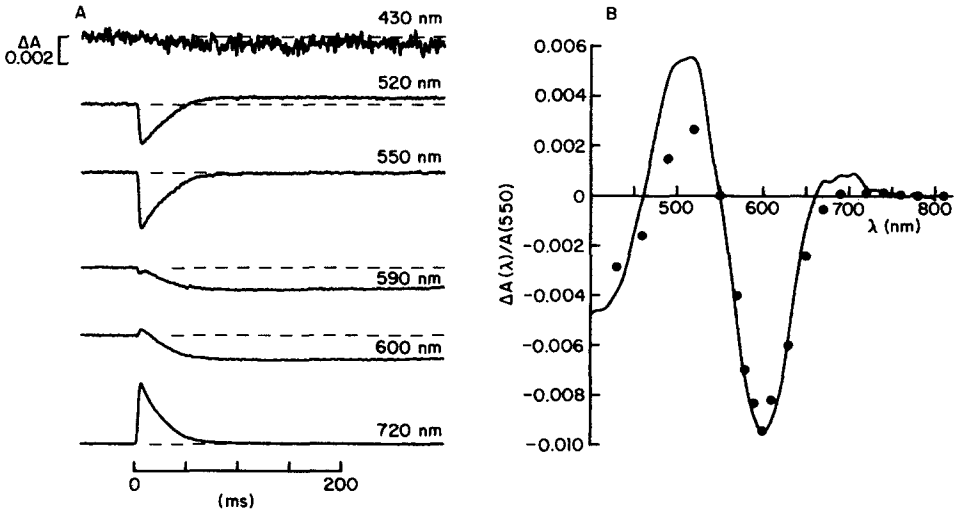

FIGURE 1. Wavelength dependence of the slowly recovering component of the antipyrylazo III absorbance change after a single action potential. (*A*) Changes in indicator-related absorbance, measured with 10-nm bandpass filters (including the 720-nm trace) at the wavelengths indicated. Each trace was recorded after a single stimulus; signal averaging was not used. (*B*) The average value of $\Delta A(\lambda)/A(550)$, in the period 200–300 ms after stimulation, plotted as a function of wavelength. The continuous curve was taken from Fig. 16 *C* in Baylor et al. (1986), and scaled to match the experimental point at 600 nm; it represents a Mg-difference spectrum obtained with 0.4 mM antipyrylazo III at pH 6.9, $0 \leqq$ free [Mg] $\leqq 1.91$ mM. Fiber 062184.2; sarcomere spacing, 4.0 μm; indicator concentration, 1.08–1.10 mM; time after saponin treatment, 157–178 min; temperature, 18.8–19.1°C; mode 1 recording. Additional information for this and other fibers containing antipyrylazo III is given in Table I in Maylie et al. (1987*c*).

Amplitude of the ΔA(590) Signal after Single Action Potential Stimulation

During the first 1–2 h of $\Delta A(590)$ measurements in a cut fiber experiment, the amplitude of the $\Delta A(590)/A(550)$ signal measured 200–300 ms after an action potential progressively increased by a factor of 2–3 (not shown). This may be related to the progressive increase in duration of the Ca signal that occurs during this same period (Maylie et al., 1987*c*). We therefore wanted to measure the $\Delta A(590)$ signal early in an experiment when the Ca signal was brief and the condition of the fiber had changed minimally from the time that saponin was applied to permeabilize the end-pool segments.

The measurements in Table I were made early in experiments on fibers that contained the minimal amount of antipyrylazo III (~0.3 mM) necessary for adequate resolution of indicator-related changes in absorbance. Column 2 gives the values of $\Delta A(590)/A(550)$ measured 200–300 ms after an action potential. The magnitude of each $\Delta A(590)$ signal has been normalized by $A(550)$, which is proportional to the indicator concentration, because, in cuvette calibrations, $\Delta A(590)/A(550)$ is directly proportional to changes in free [Mg] for the range of indicator concentrations used in this paper (Rios and Schneider, 1981; see Methods and pages 603 and 604). The

TABLE I

Amplitude of the $\Delta A(590)$ Signals after Action Potential Stimulation of Cut Fibers that Contain ~0.3 mM Antipyrylazo III

1 Fiber reference	2 $\Delta A(590)/A(550)$	3 Δ[Mg]	4 ΔpH
	$\times 10^{-3}$	μM	
061484.2	−3.86	58	0.0097
062184.2	−5.35	80	0.0134
062284.1	−3.58	54	0.0090
062584.1	−3.07	46	0.0077
062684.1	−2.74	41	0.0069
070584.1	−3.30	50	0.0083
071184.2	−2.32	35	0.0058
092484.1	−2.07	31	0.0052
111684.1	−1.80	27	0.0045
Mean	−3.12	47	0.0078
SE of mean	0.36	5	0.0009

Column 1 gives the fiber reference. Column 2 gives the average value of indicator-related $\Delta A(590)/A(550)$ during the period from 200 to 300 ms after stimulation. Columns 3 and 4 give corresponding values of Δ[Mg] and ΔpH calculated by multiplying the values in column 2 by −15 mM and −2.5 pH units, respectively (see Methods). The measurements were made 35–89 min (average value, 62 min) after the end-pool segments of the fibers were permeabilized by a 2-min exposure to a 0.01% saponin solution (Irving et al., 1987). The average concentration of antipyrylazo III inside the fiber at the optical recording site was 0.31 mM (range, 0.26–0.34 mM). The Ca signals recorded from these fibers were similar to those listed in Table IV of Maylie et al. (1987*c*): the average half-width of the indicator-related $\Delta A(720)$ signal was 10.6 ms (range, 8.9–12.4 ms), the average peak amplitude of the $\Delta A(720)$ signal corresponded to 2.82 μM free [Ca] (range, 2.16–3.42 μM) if all the indicator was able to react with Ca as in cuvette calibrations, and 36.3 μM (range, 11.0–77.2 μM) if only freely diffusible indicator was able to so react. The average temperature was 18.1°C.

average value of $\Delta A(590)/A(550)$, -3.12×10^{-3}, is similar to values reported for intact fibers, -2.5 to -3.1×10^{-3} (from the fiber used in Fig. 11 of Baylor et al., 1982*b*) and -4.0×10^{-3} (from the fiber used in Fig. 4 of Baylor et al., 1985). This similarity may be somewhat fortuitous since some of the possible differences between cut and intact fibers might affect the amplitude of the $\Delta A(590)/A(550)$ signal. These differences include the concentrations of parvalbumin (see page 603) and of phosphocreatine (see page 602) at the optical recording site and the duration of the [Ca] transient after an action potential (Maylie et al., 1987*c*).

If the absorbance change in Table I, column 2 were due solely to a change in free [Mg], and if all the intracellular antipyrylazo III were able to react with Mg as in cuvette calibrations, the average increase in free [Mg] would be 47 μM (column 3). If the signal were due solely to a change in pH, it would correspond to an average increase of 0.0078 pH units (column 4).

Effect of Repetitive Stimulation on the Amplitude and Recovery of the $\Delta A(590)$ Signal

Fig. 2 shows $\Delta A(720)$, or Ca, signals (middle traces) and $\Delta A(590)$ signals (bottom traces) associated with one, five, and ten action potentials (top traces). The Ca signal

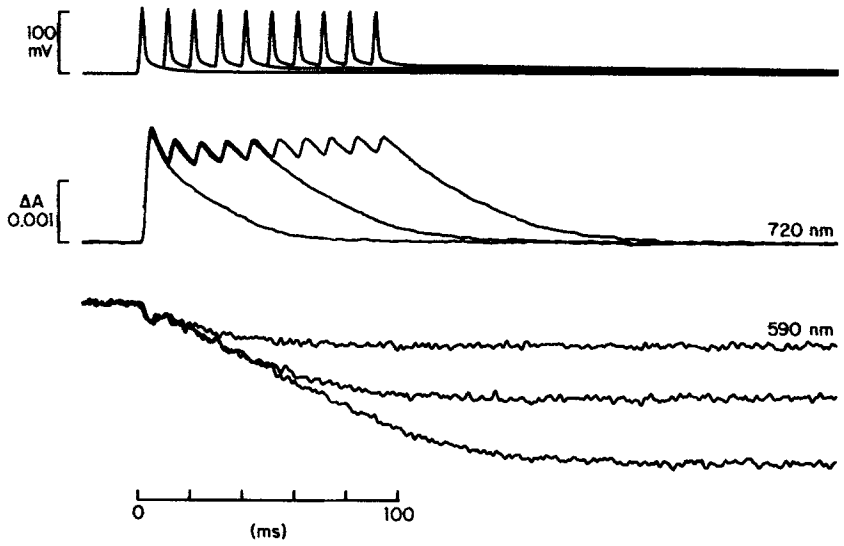

FIGURE 2. Effect of repetitive stimulation on the $\Delta A(720)$ and $\Delta A(590)$ signals. The fiber was stimulated at 100 Hz to give one, five, or ten action potentials; the actual amplitude of the first action potential, before attenuation by the 0.625-kHz eight-pole Bessel filter, was 145 mV (cf. Irving et al., 1987). The upper traces show the three superimposed action potential records, the middle traces show the $\Delta A(720)$ signals, and the bottom traces show the $\Delta A(590)$ signals. Fiber 092684.1; sarcomere spacing, 4.1 μm; antipyrylazo III concentration, 0.79–0.82 mM; time after saponin treatment, 103–111 min; temperature, 16.9°C; mode 1 recording.

did not summate during 100-Hz stimulation, which is in agreement with previous results from intact fibers (Quinta-Ferreira et al., 1984) and from cut fibers (Maylie et al., 1987*c*). On the other hand, the $\Delta A(590)$ signal did summate during repetitive stimulation. The period during which $\Delta A(590)$ continued to decrease appears to be correlated with the period during which myoplasmic [Ca] was elevated. Such an effect may contribute to the progressive increase in the amplitude of the $\Delta A(590)/A(550)$ signal during the course of cut fiber experiments, which was described in the preceding section, since the duration of the Ca transient also increases progressively (Maylie et al., 1987*c*).

After stimulation, the $\Delta A(590)$ signal recovers towards the prestimulus baseline on a time scale slower than that shown in Fig. 2. Fig. 3 shows $\Delta A(590)$ signals after one, five, and ten action potentials, taken with a slow sampling rate ~10 min after those in Fig. 2. Recovery of $\Delta A(590)$ was only partially complete 7–8 s after stimulation. A single exponential function plus a constant was fitted to the recovery phase of each trace with an iterative least-squares computer program. The theoretical curves show these fits, plotted (but not fitted) from times before the peaks. The rate constants were 0.56, 0.62, and 0.66 s^{-1} after one, five, and ten action potentials, respectively.

Table II gives information about the peak amplitude and recovery of $\Delta A(590)$ signals in four fibers. Columns 4 and 5 give, respectively, the peak amplitudes of

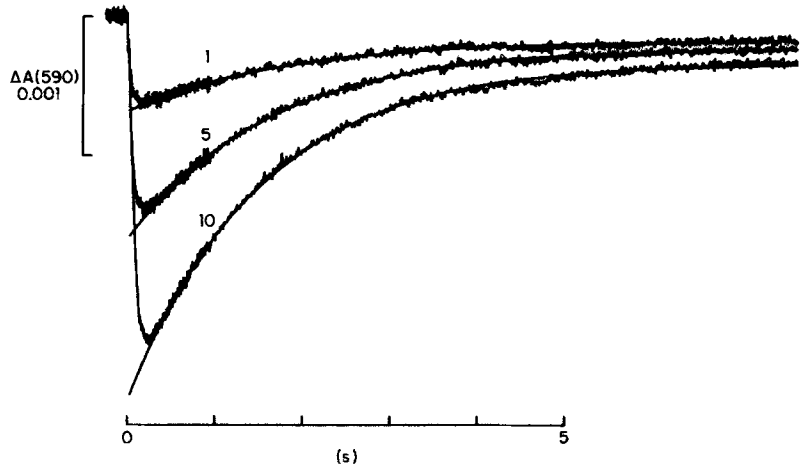

FIGURE 3. Recovery of the $\Delta A(590)$ signal after stimulation at 100 Hz to give one, five, or ten action potentials (as indicated). These traces were taken with a slow sampling rate ~10 min after those in Fig. 2; mode 1 recording was used. The indicator concentration was 0.74–0.76 mM and the temperature was 16.8°C. The smooth curves represent theoretical fits of a single exponential plus a constant to the recovery phase of the traces. The best-fit rate constants were 0.56 (one action potential), 0.62 (five action potentials), and 0.66 s^{-1} (ten action potentials). The fitted steady levels of $\Delta A(590)/A(550)$ were −0.00167 (one action potential), −0.00227 (five action potentials), and −0.00332 (ten action potentials).

$\Delta A(590)/A(550)$ associated with a single action potential and the value 7–7.7 s after stimulation. The signal amplitudes in column 4 are larger than those in column 2 of Table I, mainly because they were obtained later in the experiment. Column 6 gives the rate constant of the exponential function fitted to the $\Delta A(590)$ recovery. Columns 7–9 give corresponding parameters from traces associated with ten-action-potential stimulation. Three fibers were studied with both one and ten-action-potential stimulation. In these fibers, the peak amplitude of $\Delta A(590)/A(550)$ after ten action potentials was 3.7–4.6 times the corresponding value after one action potential. In addition, the recovery rate constant appeared to be slightly larger after ten action potentials than after one.

Comparison of the Time Courses of the Antipyrylazo III ΔA(590) Signal and the Myoplasmic pH Transient

In both cut and intact fibers at 18°C, the antipyrylazo III Ca signal returns to near the prestimulus baseline by 0.2 s after a single action potential. At this time, the 590-nm signal has reached its peak value (see Fig. 1 *A* for cut fiber results and Baylor et al., 1982*b*, 1983*b*, 1985 for intact fiber results). Thereafter, it recovers slowly over the next few seconds (Fig. 3). The wavelength dependence of the slowly recovering component of the absorbance change matches approximately the cuvette difference spectra for increases in either pH or free [Mg] (Fig. 1 *B*; Baylor et al., 1982*b*, 1985), which are similar but not identical. The amplitude of the slowly recovering signal, however, is relatively small, at least after a single action potential, so

TABLE II

Peak Amplitude and Recovery of the ΔA(590) Signal after One and Ten Action Potentials

1	2	3	4	5	6	7	8	9
			ΔA(590)/A(550), 1 AP			ΔA(590)/A(550), 10 AP		
Fiber reference	Time after saponin	Indicator concentration	Peak	Late	Rate constant	Peak	Late	Rate constant
	min	*mM*	$\times 10^{-3}$	$\times 10^{-3}$	s^{-1}	$\times 10^{-3}$	$\times 10^{-3}$	s^{-1}
062184.2	204–209	0.97–0.99	−8.75	−1.88	0.64	−40.07	−3.58	0.81
071184.2	104–111	1.06–1.10	−5.91	−2.10	0.67	−22.01	−3.94	0.73
092684.1	121–129	0.73–0.76	−6.07	−1.60	0.55	−23.63	−3.34	0.66
111684.1	70–71	0.74–0.75	−2.90	−1.75	0.33	—	—	—
Mean			−5.91	−1.83	0.55	−28.57	−3.62	0.73
SE of mean			1.20	0.11	0.08	5.77	0.17	0.04

Column 1 gives fiber reference and column 2 gives the time that elapsed from saponin treatment of the end-pool segments to the time of the measurements used for columns 3–9. Column 3 gives the concentration of antipyrylazo III at the optical site. Columns 4–6 give information about the ΔA(590)/A(550) signal after a single action potential. Column 4 gives the peak value, column 5 gives the approximately steady level reached 7–7.7 s after the action potential, and column 6 gives the rate constant of an exponential function fitted, plus a constant, to the recovery time course. Columns 7–9 give similar information about the signal after ten action potentials at 100 Hz. In fiber 062184.2, the Ca signal summated (the amplitude of the tenth Ca signal was 1.8 times that of the first) whereas in fibers 071184.2 and 092684.1 it did not. The presence of summation in fiber 062184.2 may be due to the long interval between saponin treatment of the end-pool segments and the measurement (Maylie et al., 1987*c*). The average temperature was 18.3°C.

that estimates of its wavelength dependence are sensitive to small errors in the intrinsic correction. Consequently, it is difficult to determine, solely on the basis of spectral information, whether the signal is due to a change in [Mg] or pH.

To help resolve this uncertainty, a few experiments were carried out in which phenol red and Me_2CF were used to monitor changes in myoplasmic pH after action potential stimulation. The time course of indicator appearance at the optical recording site, after the addition of 1–3 mM indicator to the end-pool solutions, was fitted by equations for diffusion plus linear reversible binding (Maylie et al., 1987*b*). According to this analysis, ~0.7 of the phenol red inside a fiber was bound to or taken up by intracellular constituents; the corresponding fraction for Me_2CF was 0.8.

With either phenol red or Me_2CF, the amplitude of the pH signal after an action potential (Eq. 5 or 6) decreased considerably during the first hour of a cut fiber experiment, although the time course of the signal showed little change and the action potential and holding current remained constant and normal. The decrease in the amplitude of the pH signals was apparent in the first reliable records of changes in indicator-related absorbance. The amplitude of our earliest ΔpH signals were estimated, as described in Methods, to be 0.004 and 0.008 with phenol red (42 and 32 min after saponin treatment, respectively) and 0.040 and 0.033 with Me_2CF (36 and 41 min after saponin treatment, respectively). The magnitude of ΔpH in a freshly prepared cut fiber cannot be estimated reliably by extrapolating our data. With phenol red, the early stages of this decrease in the pH signal, to about half its initial value, were accompanied by little change in either the amplitude or time course of the intrinsic retardation signal, which was normal. The retardation signal is thought to be closely related to the Ca transient (Suarez-Kurtz and Parker, 1977; Baylor et al., 1982*b*; Baylor and Hollingworth, 1987; Maylie et al., 1987*c*). With Me_2CF, the decrease in amplitude of the pH signal was accompanied by a decrease in amplitude of the retardation signal and both signals disappeared within 30 min of the addition of indicator to the end-pool solutions. Since the action potential and holding current remained normal, this suggests that Me_2CF blocked excitation-contraction coupling. This blocking effect was observed in both fibers studied and was not investigated further.

Fig. 4 *A* compares the time course of the pH signals with that of the antipyrylazo III $\Delta A(590)$ signal; the signals have been scaled to have the same peak value. The top trace shows an action potential (from Fig. 2). The next superimposed traces show two pH signals, one recorded early in an experiment on a fiber containing phenol red (λ = 570 nm) and the other recorded early from a fiber containing Me_2CF (λ = 510 nm). These are plotted so that an upward deflection corresponds to an increase in pH. In each case, a simultaneous recording was made of the absorbance change at the isosbestic wavelength of the indicator, 480 nm for phenol red and 470 nm for Me_2CF. These traces were flat (not shown), which is consistent with the idea that the two superimposed signals in Fig. 4 *A* arise from changes in pH.

Each pH signal in Fig. 4 *A* shows a transient increase in pH, possibly due to protons entering the sarcoplasmic reticulum accompanying Ca release (Somlyo et al., 1981; Baylor et al., 1982*a*; Baylor et al., 1987). The rise time and duration of the transients are different for the two indicators. This is surprising since the action potential and the active retardation signal were normal and similar in both fibers, and in each fiber these signals were similar to those measured before the addition of indicator to the end pools. The most likely explanation of the difference in time course of the phenol red and Me_2CF signals is that the indicators are bound or sequestered inside a muscle fiber at different locations that undergo temporally different changes in pH.

The lowermost trace in Fig. 4 *A* shows the $\Delta A(590)$ signal from Fig. 2, plotted with inverted polarity to facilitate comparison of the time courses (an upward deflection would now be produced by an increase in pH or free [Mg]). After the initial transient component, the early change in antipyrylazo III absorbance at 590 nm is delayed compared with either of the pH signals and, unlike them, shows negligible recovery by 0.2 s after the stimulus.

Fig. 4 *B* shows the phenol red pH signal recorded with a slow sampling rate and the antipyrylazo III $\Delta A(590)$ signal recorded on the same time scale (from Fig. 3, inverted polarity). The time courses are obviously different. The pH signal shows partial recovery within the first 0.4 s and then slowly increases to 0.7 times the early peak value at 7–7.7 s; this slow alkalinization may be partly due to the net break-

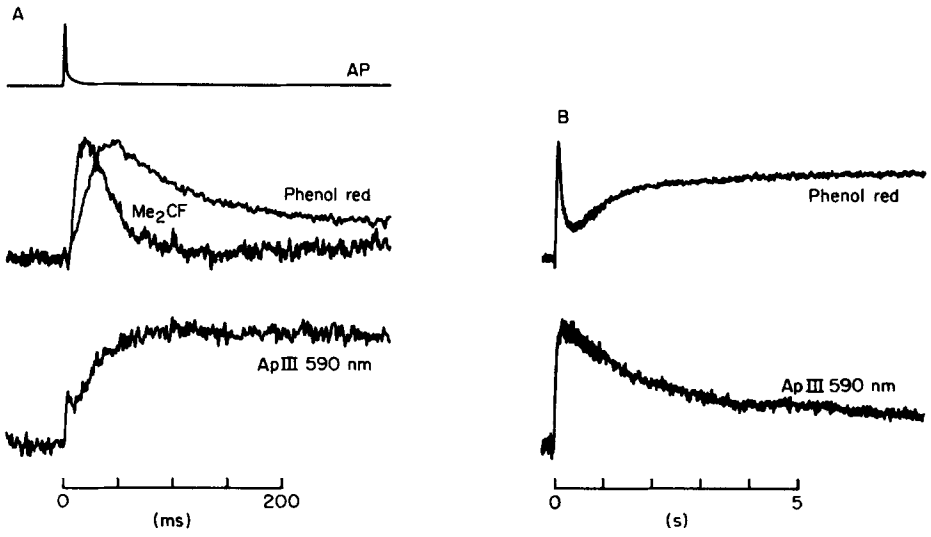

FIGURE 4. Comparison of the time courses of two pH signals, from phenol red and Me_2CF, and of the $\Delta A(590)$ signal from antipyrylazo III after single action potential stimulation. The optical traces, from three different fibers, each containing a different indicator, have been arbitrarily scaled to the same peak value. (*A*) The top trace shows an action potential (from Fig. 2). The next two superimposed traces show the pH signals. The phenol red signal was recorded from fiber 102284.2; diameter, 98 μm; sarcomere spacing, 4.1 μm; action potential amplitude, 128 mV; indicator concentration, 1.36 mM; time after saponin treatment, 32 min; time after addition of indicator to the end-pool solutions, 11 min; mode 2 recording. The Me_2CF signal was recorded from fiber 102384.2; diameter, 73 μm; sarcomere spacing, 4.1 μm; action potential amplitude, 135 mV; indicator concentration, 0.18 mM; time after saponin treatment, 41 min; time after addition of indicator to the end-pool solutions, 18 min; mode 2 recording. The bottom trace shows the 590-nm signal from antipyrylazo III (from Fig. 2, plotted with inverted polarity). (*B*) Slow changes in the phenol red pH signal (mode 2 recording with 5.66-mM indicator, 22 min after the phenol red signal in *A*) and in the $\Delta A(590)$ signal from antipyrylazo III (from Fig. 3, plotted with inverted polarity). An attempt was also made to record the Me_2CF pH signal with a slow sampling rate. This was unsuccessful owing to a drift in the baseline absorbance which may be related to indicator bleaching. Temperature range, 16.8–18.2°C.

down of phosphocreatine resulting from the action of the sarcoplasmic reticulum Ca pump (see page 132 in Baylor et al., 1982*a*). After 0.2 s, the $\Delta A(590)$ signal slowly decreases to 0.26 times peak value at 7–7.7 s.

The conclusion from the comparisons shown in Fig. 4 is that the time course of the myoplasmic pH transient is qualitatively different from that of the change underlying the $\Delta A(590)$ signal. The main differences are that (*a*) 300 ms after stim-

ulation, the pH signals show at least two-thirds recovery whereas the $\Delta A(590)$ signal shows almost no recovery (Fig. 4 *A*), and (*b*) from 0.5–7 s after stimulation, the phenol red signal shows an increase in pH whereas the $\Delta A(590)$ signal, if due to a change in pH, shows a decrease. If the $\Delta A(590)$ signal reflects an increase in either pH or free [Mg], as suggested by the wavelength dependence of this component of the antipyrylazo III absorbance change, the main part of the signal is likely to be due to an increase in free [Mg]. The component of the $\Delta A(590)$ signal that is maintained after 7 s, however, may be due to a long lasting increase in either free [Mg] or pH or both.

Changes in $\Delta A(590)$ Associated with Voltage-Clamp Depolarizations

Changes in antipyrylazo III absorbance were also measured under voltage-clamp conditions. Fig. 5 shows traces associated with 100-ms depolarizing pulses to −50, −40, and −20 mV, from a holding potential of −90 mV. The top set of traces shows the voltage, and the lower sets show the simultaneously recorded $\Delta A(720)$, $\Delta A(590)$, and $\Delta A(810)$ signals. The $\Delta A(720)$ and $\Delta A(590)$ traces have been corrected for intrinsic fiber contributions. The $\Delta A(590)$ signal was larger for greater depolarizations, and it continued to increase during the period when the $\Delta A(720)$, or Ca, signal was above baseline. This dependence on myoplasmic free [Ca] is similar to that seen with repetitive action potential stimulation (Fig. 2). The amplitude of the slowly recovering component of the absorbance change, measured after repolarization, when the Ca signal had returned to baseline, was found to vary with wavelength in a manner similar to that shown in Fig. 1 *B* (not shown).

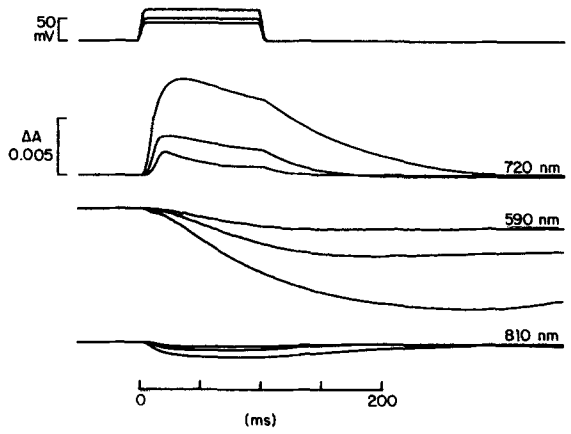

FIGURE 5. Antipyrylazo III $\Delta A(720)$ and $\Delta A(590)$ signals under voltage-clamp conditions. The top set of superimposed records shows voltage recorded during three 100-ms pulses to −50, −40, and −20 mV from a holding potential of −90 mV. The next three sets of traces show the corresponding indicator-related $\Delta A(720)$, indicator-related $\Delta A(590)$, and $\Delta A(810)$ signals. Fiber 101984.2; sarcomere spacing, 3.7 μm; time after saponin treatment, 116–120 min; time after indicator addition to the end pools, 98–102 min; indicator concentration, 0.88–0.89 mM; temperature, 18.7°C; mode 1 recording.

Fig. 5 shows only the early part of records taken with a slow sampling rate. Fig. 6 shows the entire $\Delta A(590)$ traces. After an initial peak, shortly after repolarization,

the 590-nm signals returned slowly towards the baseline level. These changes are similar to those shown in Fig. 3 after repetitive action potential stimulation. A single exponential function plus a constant was least-squares fitted to the recovery phase of each $\Delta A(590)$ signal. The theoretical curves, also shown in Fig. 6, give a good fit to the $\Delta A(590)$ records. The exponential rate constants were 0.61 s^{-1} after the depolarization to −50 mV, 0.74 s^{-1} after the depolarization to −40 mV, and 0.78 s^{-1} after the depolarization to −20 mV. These rate constants are similar to those obtained in Fig. 3.

The depolarizations used in Figs. 5 and 6 were relatively brief and the $\Delta A(590)$ signal did not reach a steady level during the depolarization. In two other fibers, depolarizations lasting 1–2 s were applied. Panels *A* and *B* of Fig. 7 show traces of voltage (top), $\Delta A(720)$ (middle), and $\Delta A(590)$ (bottom) from these two fibers. In each fiber, the largest depolarizations produced large decreases in 590-nm absorbance that almost reached steady-state levels during the pulse. Recovery after the pulses was similar to that observed in Figs. 3 and 6.

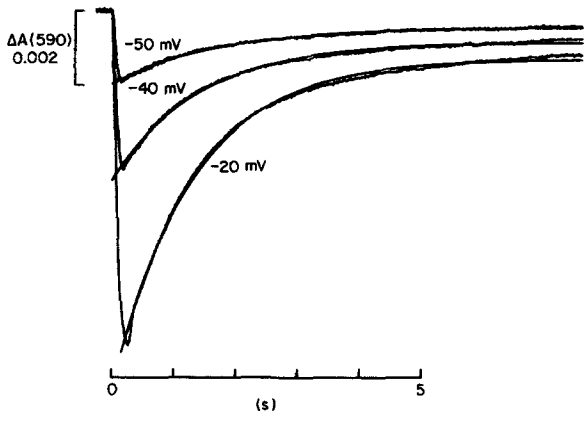

FIGURE 6. Recovery of $\Delta A(590)$ signals after a 100-ms depolarization under voltage clamp. These are from the same traces as in Fig. 5, but plotted on a slow time base so that all the data points could be shown. The theoretical curves represent fits by a single exponential function plus a constant, determined by a least-squares computer routine; the fitted rate constants were 0.61 (−50 mV), 0.74 (−40 mV), and 0.78 s^{-1} (−20 mV).

Panels *A* and *B* of Fig. 8 show expanded plots of the development of the $\Delta A(590)$ signals from the corresponding panels in Fig. 7. An exponential function plus a constant was least-squares fitted to each trace and the fitted curves are also plotted; the final levels given by the fits are indicated by horizontal tick marks to the right of each trace. In the experiment in *A*, the exponential rate constants were 0.78, 1.01, 3.10, and 3.70 s^{-1} during depolarizations to −50, −40, −30, and −20 mV, respectively. The values in *B* were 0.95, 1.25, 1.82, and 2.64 s^{-1} during depolarizations to −55, −50, −40, and −20 mV, respectively. In both experiments the rate constant increased as the voltage was made more positive.

The results of voltage-clamp experiments on five fibers are summarized in Table III. Column 6 gives the peak value of the $\Delta A(590)/A(550)$ signal and column 7 gives its value at 7–7.7 s after the start of the depolarization. If all the signal arises from an increase in myoplasmic free [Mg], the peak increases associated with the largest depolarizations are of the order of 1 mM.

Columns 8 and 9 of Table III give the rate constants of exponential functions

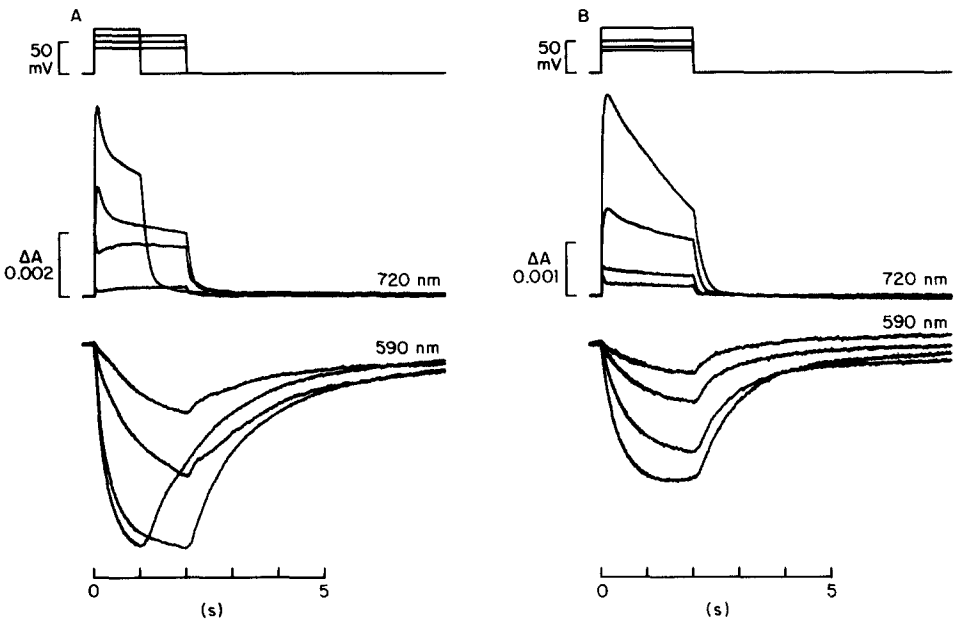

FIGURE 7. $\Delta A(720)$ and $\Delta A(590)$ signals associated with 1–2-s depolarizations under voltage clamp. The top sets of records show voltage, the middle sets show indicator-related $\Delta A(720)$, and the bottom sets show indicator-related $\Delta A(590)$. (A) Fiber 112184.2; sarcomere spacing, 3.9 μm; time after saponin treatment, 102–131 min; time after addition of indicator to the end pools, 86–115 min; indicator concentration, 0.72–0.78 mM; temperature, 18.1°C; mode 1 recording. (*B*) Fiber 111584.1; sarcomere spacing, 4.1 μm; time after saponin treatment, 201–213 min; time after adding indicator to the end pools, 178–190 min; indicator concentration, 0.52–0.55 mM; temperature, 17.7°C; mode 1 recording.

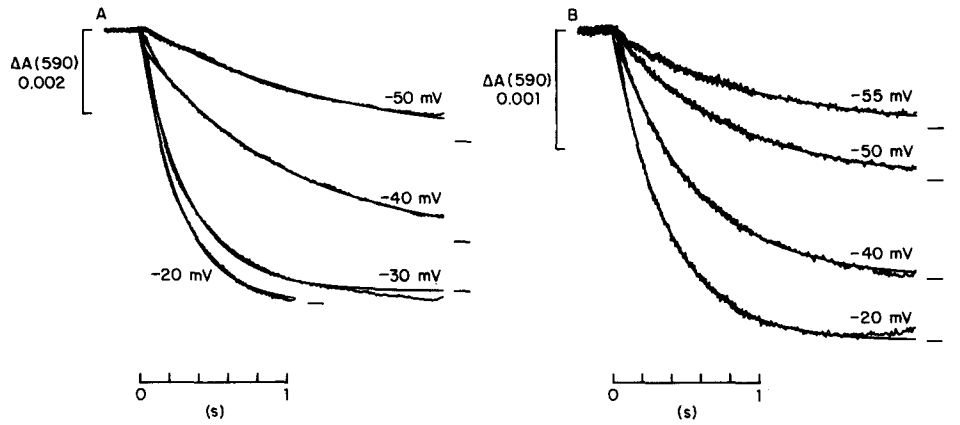

FIGURE 8. $\Delta A(590)$ signals recorded during 1–2-s depolarizations to the voltages shown. The traces are the same as those shown in Fig. 7 but plotted on an expanded time base. Each theoretical curve represents an exponential function plus a constant, least-squares fitted to each experimental trace, with the final level indicated to the right of each curve. (*A*) The rate constants are 0.78, 1.01, 3.10, and 3.70 s^{-1} during depolarizations to −50, −40, −30, and −20 mV, respectively. (*B*) The rate constants are 0.95, 1.25, 1.82, and 2.64 s^{-1} for depolarizations to −55, −50, −40, and −20 mV, respectively.

TABLE III

Properties of the ΔA(590) Signal Associated with Voltage-Clamp Depolarizations

1	2	3	4	5	6	7	8	9
					ΔA(590)/A(550)			
Fiber reference	Time after saponin	Indicator concentration	Duration	Voltage	Peak	Late	ON rate constant	OFF rate constant
	min	*mM*	*ms*	*mV*	$\times 10^{-3}$	$\times 10^{-3}$	s^{-1}	s^{-1}
101984.2	120	0.88	100	−50	−12.1	−2.8		0.61
	118	0.89	100	−40	−27.2	−5.0		0.74
	116	0.89	100	−20	−57.2	−7.6		0.78
Mean								0.71
111384.2	134	1.24	100	−20	−74.1	−9.1		0.76
	131	1.22	500	−20	−93.0	−10.5		0.75
Mean								0.76
111584.1	213	0.52	2000	−55	−16.1	−2.6	0.95	1.28
	209	0.53	2000	−50	−25.1	−3.7	1.25	0.80
	205	0.54	2000	−40	−43.6	−7.9	1.82	1.03
	197	0.57	100	−20	−25.4	−1.5		1.05
	188	0.59	500	−20	−44.2	−1.6		1.04
	192	0.58	1000	−20	−52.0	−2.2	2.88	1.01
	201	0.55	2000	−20	−52.9	−4.2	2.64	0.99
	217	0.51	1000	0	−54.4	−6.6	2.44	1.00
Mean								1.03
111684.2	82	0.75	100	−40	−9.3	−3.7		0.90
	103	0.83	100	−40	−10.1	−2.8		0.61
	69	0.65	200	0	−39.1	−5.6		0.69
	112	0.87	200	0	−62.0	−5.3		0.77
Mean								0.74
112184.2	93	0.78	2000	−50	−16.5	−8.0		0.44
	106	0.78	2000	−50	−22.5	−11.2		0.48
	114	0.78	2000	−50	−22.3	−6.5		0.43
	131	0.72	2000	−50	−22.1	−7.0	0.78	0.74
	102	0.78	2000	−40	−40.2	−14.2	1.01	0.59
	128	0.73	2000	−40	−46.8	−10.1	1.69	0.79
	125	0.75	2000	−30	−65.0	−11.8	3.10	0.76
	110	0.78	1000	−20	−60.4	−9.0	3.70	0.68
Mean								0.61

Column 1 gives fiber reference and column 2 gives the time that elapsed from saponin treatment of the end-pool segments to the time of the measurements. Column 3 gives the concentration of antipyrylazo III at the optical site. Columns 4 and 5 give, respectively, the duration of, and the voltage during the depolarizing voltage-clamp pulse. Columns 6–9 give information about ΔA(590)/A(550). Column 6 gives the peak value, column 7 gives the average level reached 7–7.7 s after the start of the depolarization, column 8 gives the rate constant of an exponential function fitted to the onset time course of the ΔA(590) signal during a 1–2 s depolarization, and column 9 gives the rate constant fitted to the recovery time course after repolarization. The temperature was 17.7–18.9°C.

least-squares fitted to the onset (i.e., during depolarization) and recovery (i.e., after repolarization) time courses, respectively. The values in column 8 show that there was an increase in the ON rate constant as the voltage (column 5) was made more positive. On the other hand, there is no obvious correlation between the value of the recovery rate constant (column 9) and the voltage of the depolarizing pulse (col-

umn 5). In column 9, the average recovery rate constant for each fiber is indicated below the individual measurements. These values, ranging from 0.61 to 1.03 s^{-1}, are similar to those observed after action potential stimulation (columns 6 and 9 in Table II).

DISCUSSION

After action potential stimulation of a cut muscle fiber containing antipyrylazo III, there is a change in indicator absorbance that has two components with different time courses and wavelength dependences: an early transient component, due to an increase in myoplasmic free [Ca] (Maylie et al., 1987*c*), and a second, more slowly developing component that recovers towards baseline about 100 times more slowly than the Ca transient (Figs. 1–3). Although the wavelength dependence of the slowly developing component is consistent with an increase in either free [Mg] or pH, its time course is clearly different from that of the pH signals obtained with two different pH indicators (Fig. 4). This strongly suggests that this component of the antipyrylazo III signal is due primarily to an increase in myoplasmic free [Mg], with a possible small contribution from a change in pH.

The Origin of the Myoplasmic Mg Transient

Since Mg was not used in the Ringer's and TEA solutions bathing the fibers, the increase in myoplasmic free [Mg] must be due to Mg leaving intracellular compartments or myoplasmic buffers. It seems unlikely that the sarcoplasmic reticulum participates in this increase since it appears to gain, not lose, Mg during activity; after a 1.2-s tetanus, the Mg content of the sarcoplasmic reticulum is slightly increased (Somlyo et al., 1981). Mitochondria are also an unlikely candidate since they occupy only 1% of the fiber volume (Mobley and Eisenberg, 1975) and their Mg content is unchanged after a 1.2-s tetanus (Somlyo et al., 1981). It seems more likely that the source of the Mg is a myoplasmic Mg buffer, such as phosphocreatine or parvalbumin.

Phosphocreatine binds Mg more tightly than does creatine so that phosphocreatine splitting should lead to a release of Mg. Since HPO_4^{2-} can also bind Mg, and with a dissociation constant that is similar to that of phosphocreatine (20 mM for HPO_4^{2-}, Smith and Martell, 1976; 25 mM for phosphocreatine, O'Sullivan and Perrin, 1964), some of the Mg that is released from phosphocreatine will be complexed with the HPO_4^{2-} component of the phosphate that is liberated. After a single action potential in a highly stretched intact fiber, the associated increase in free [Mg] is estimated to be 0.0024 times the resting free [Mg] if the Mg buffering action of HPO_4^{2-} is neglected (page 133 of Baylor et al., 1982*a*) and less if the buffering action is included. This estimate of Δ[Mg] is expected to be reduced further in cut fibers, owing to a reduction in the concentration of phosphocreatine due to diffusional equilibration with the end-pool solutions (see page 602); the concentration of phosphocreatine in the end-pool solutions was 20 mM (Table I in Irving et al., 1987) whereas that inside an intact fiber is ~50 mM (Godt and Maughan, 1988). Thus, Mg release associated with phosphocreatine splitting should increase free [Mg] by no more than 1 μM or so after a single action potential and, therefore, should make only a small contribution to the increase estimated from the present

results, on average 47 μM early in a cut fiber experiment (Table I, column 3) and two to three times that after 1–2 h (page 589).

It seems likely that most of the observed increase in myoplasmic free [Mg] is due to Mg leaving parvalbumin (Baylor et al., 1983*a*, 1985), a Ca and Mg binding protein found in brain (Gosselin-Rey et al., 1978) and fast twitch skeletal muscle (for example, Gosselin-Rey and Gerday, 1977), which is thought to play a role in muscle relaxation (Gerday and Gillis, 1976).

Properties of the Mg Signal that Are Consistent with Mg Dissociation from Parvalbumin

Many properties of the $\Delta A(590)$, or Mg, signal are consistent with the idea that it is due to Mg dissociating from and subsequently rebinding to parvalbumin. If the two Ca,Mg sites on parvalbumin are identical and noninteracting (Potter et al., 1977; Haiech et al., 1979), the simplest reaction scheme for divalent cation complexation can be written

$$\mathrm{Mg} + \mathrm{Parv} \underset{k_{-1}}{\overset{k_1}{\rightleftharpoons}} \mathrm{MgParv},$$

$$\mathrm{Ca} + \mathrm{Parv} \underset{k_{-2}}{\overset{k_2}{\rightleftharpoons}} \mathrm{CaParv}.$$

CaParv and MgParv represent parvalbumin sites that are complexed with Ca and Mg, respectively, and Parv represents a parvalbumin site that is divalent cation-free; k_1 and k_2 are forward rate constants, as indicated; k_{-1} and k_{-2} are backward rate constants.

After stimulation, when free [Ca] is elevated, equilibrium binding favors Ca over Mg; consequently, [MgParv] should decrease, leading to an increase in free [Mg]. Later, after free [Ca] has returned to its resting level, these changes should reverse. The results reported here are consistent with these predictions. During either repetitive action potential stimulation or voltage-clamp depolarization, $\Delta A(590)$ continued to decrease (implying that [Mg] continued to increase) during the period when [Ca] was elevated, even during periods when [Ca] was constant or slowly decreasing (Figs. 2, 5, and 7). After [Ca] had returned close to its baseline level, [Mg] slowly decreased (Figs. 3, 6, and 7).

According to the above scheme, the kinetics of changes in free [Mg], and consequently of the $\Delta A(590)$ signal, depends on free [Ca], free [Mg], and the rate constants k_1, k_{-1}, k_2, and k_{-2}. After stimulation, if free [Ca] is sufficiently large, some of the Mg that was bound to parvalbumin at rest is replaced by Ca. If a high [Ca] level is maintained, as in our experiments with prolonged strong depolarizations under voltage clamp, Δ[Mg] should approximately follow an exponential time course determined by the rate constant for Mg dissociating from parvalbumin, k_{-1}. In two experiments at 18–19°C (Figs. 7 and 8), the rate constant of the exponential fitted to the Mg signal appeared to increase with increasing levels of free [Ca] and to saturate at values of ~3 and 4 s^{-1} for the largest depolarizations studied (column 8 in Table III). These rate constants are similar to the values of k_{-1} obtained by direct measurements on isolated parvalbumin carried out at somewhat higher tempera-

tures: k_{-1} = 6 s^{-1} for carp parvalbumin at 25°C (Johnson et al., 1981) and 3.5–6 s^{-1} for bullfrog parvalbumins PA-1 and PA-2 at 20°C (Ogawa and Tanokura, 1986).

During recovery, when free [Ca] is very small, Ca dissociates from parvalbumin with a rate constant k_{-2} and is replaced by Mg. In this case, changes in free [Mg] should approximately follow a single exponential function with a rate constant that is close to the value of k_{-2}. After repolarization, under both action potential and voltage-clamp conditions, the Mg signal returns towards the baseline level with an average rate constant between 0.5 and 1 s^{-1} (columns 6 and 9 in Table II; column 9 in Table III). This range is also similar to the values of k_{-2} measured on isolated parvalbumins: k_{-2} = 1 s^{-1} for carp parvalbumin at 25°C (Johnson et al., 1981) and 1.16–1.5 s^{-1} for bullfrog parvalbumins at 20°C (Ogawa and Tanokura, 1986).

There are several reasons why the time course of $\Delta A(590)$ might not exactly match that of Δ[Mg]. $\Delta A(590)$ contains a small contribution from the transient decrease in the concentration of the Mg:indicator complex produced by the decrease in free indicator concentration that is associated with the [Ca] transient (see pages 170 and 171 of Baylor et al., 1982*b*). It may also contain a small contribution from changes in pH (Fig. 4) or from complexation of indicator with Ca (we do not know the precise value of the isosbestic wavelength for changes in [Ca] inside a fiber and it is unlikely that our 590-nm filter is centered exactly on that wavelength).

The general conclusion of this section is that the time course of the $\Delta A(590)$ signal is broadly consistent with that expected from the kinetics of Mg and Ca complexation by parvalbumin. The following section shows that the amplitude of the $\Delta A(590)$ signal is also consistent with measurements of the myoplasmic concentration of parvalbumin inside intact fibers.

The Amplitude of Mg Signals and Estimates of Parvalbumin Concentration Inside a Cut Fiber

If the $\Delta A(590)$ signal is solely due to Mg dissociating from parvalbumin, it is possible to estimate the concentration of parvalbumin that must be involved. The largest changes in $\Delta A(590)/A(550)$ that we observed, associated with large depolarizations (Table III, column 6), correspond to increases in free [Mg] estimated to be 0.8–1.4 mM according to cuvette calibrations (see Methods). The total amount of Mg released from parvalbumin must be greater than this, because of the action of myoplasmic Mg buffers. Nearly all the Mg buffering power in the millimolar range of free [Mg] is due to phosphocreatine, which is present at a concentration of ~50 mM in an intact unfatigued frog muscle fiber (Godt and Maughan, 1988). In cut fibers, the concentration of phosphocreatine at the optical recording site should be less than this, owing to exchange with the end-pool solutions. Phosphocreatine has about the same molecular weight as tetramethylmurexide and therefore might be expected to have about the same diffusion constant inside a fiber, estimated as 1.75×10^{-6} cm^2/s at 18°C (corrected for binding or compartmentalization, Table II, column 6 in Maylie et al., 1987*a*). According to the solution of the one-dimensional diffusion equation appropriate for our experimental conditions (Eq. 6 in Maylie et al., 1987*b*), the phosphocreatine at the optical site should be 90% equilibrated with that in the end-pool solutions, in which its concentration is 20 mM, 30 min after saponin treatment of the end-pool segments of the fiber. The [Mg] mea-

surements described in this paper are therefore likely to have been made with a myoplasmic concentration of phosphocreatine of ~20 mM.

Phosphocreatine has a dissociation constant for Mg of 25 mM (O'Sullivan and Perrin, 1964). According to the standard binding equation, a 0.8–1.4 mM increase in free [Mg], above a resting level of 1 mM (taken as the concentration in the internal solution; Table I in Irving et al., 1987), would require that an additional 0.6–1.0 mM [Mg] be complexed with phosphocreatine. Consequently, the change in $\Delta A(590)/A(550)$ observed during large depolarizations would require that parvalbumin must have released 1.4–2.4 mM [Mg]. If each of the two Ca,Mg sites on parvalbumin were initially complexed with Mg and released this Mg during a large depolarization, the concentration of parvalbumin must have been 0.7–1.2 mM.

This estimate of myoplasmic parvalbumin concentration is in good agreement with recent direct measurements on tibialis anterior muscle fibers, 1.0 mM (Hou et al., 1988), and semitendinosus muscle fibers, 1.0 mM (D. W. Maughan, personal communication), both from *Rana temporaria*. These values are larger, by a factor of two, than the 0.5 mM reported by Gosselin-Rey and Gerday (1977) (which was used in the calculations of sarcoplasmic reticulum Ca release carried out by Baylor et al., 1983*a* and by Maylie et al., 1987*a*, *c*).

The agreement between our estimate of parvalbumin concentration and the measurements of Hou et al. (1988) and D. W. Maughan (personal communication) may be fortuitous. First, some of the parvalbumin inside the fiber at the optical site may have diffused along the fiber and into the end-pool solutions, particularly if the saponin treatment of the end-pool segments renders them permeable to a molecule as large as parvalbumin. Second, some of the parvalbumin sites may not have released Mg during large depolarizations, either because Mg did not occupy the site at rest or because Mg was not replaced by Ca during the period when free [Ca] was elevated. Third, there may be sources or sinks for Mg other than parvalbumin and phosphocreatine; for example, some Mg appears to enter the sarcoplasmic reticulum during a 1.2-s tetanus (Somlyo et al., 1981). Fourth, an average fraction 0.68 of the antipyrylazo III inside a cut fiber appears to be bound or sequestered or, for some other reason, unable to diffuse freely (Maylie et al., 1987*c*); this may be related to the finding that the indicator's absorbance spectrum in a resting fiber, in the wavelength range 570–670 nm, is red shifted compared with that in a cuvette (Figs. 3 and 4 in Maylie et al., 1987*c*). Such changes in the ability of antipyrylazo III to diffuse and in its resting absorbance spectrum raise the possibility that the apparent dissociation constant for Mg or the absorbance change produced by Mg complexation may be different from their cuvette values; hence, the calibration of changes in free [Mg] inside a muscle fiber may be different from that obtained in a cuvette. Any calibration errors introduced by indicator binding, however, might be smaller for Mg than for Ca (see Maylie et al., 1987*c*) because, under the conditions of our experiments, the predominant stoichiometry of Mg:indicator complexes is 1:1, whereas that of Ca:indicator complexes is 1:2 (Rios and Schneider, 1981). For example, if the bound or sequestered indicator is unable to react with Mg or Ca, the calibration estimates for small concentrations of cation would be altered by the factor (free indicator concentration)/(total indicator concentration) for Mg and by the same factor squared for Ca. It is also possible that the bound or sequestered indicator can participate in the formation of 1:1 cation:indicator complexes but not 1:2

complexes. Fifth, the use of a constant scaling factor, −15 mM, to relate $\Delta A(590)/A(550)$ to Δ[Mg] may introduce an error. Baylor et al. (1986) determined cuvette Mg-difference spectra as the difference between absorbance spectra measured with free [Mg] = 1.61–1.91 mM and those measured with [Mg] = 0 mM. The relation between $\Delta A(590)/A(550)$ and free [Mg] may not be strictly linear over the range of [Mg] from 0 mM (used for the cuvette reference spectrum) to 2–3 mM, which is the free [Mg] estimated from the largest $\Delta A(590)$ signals in our experiments (assuming that resting free [Mg] = 1 mM; see page 587).

The Role of Parvalbumin in Muscle Relaxation

After a single action potential at 18°C, the average increase in free [Mg] was 47 μM in fibers that contained 0.3 mM antipyrylazo III and were studied ~1 h after saponin treatment (Table I, column 3). If the concentration of phosphocreatine at the optical site was the same as that in the end-pool solutions (20 mM, see page 602), the 47-μM increase in free [Mg] would require an additional increase of 35 μM in the amount of [Mg] bound to phosphocreatine. Thus, if parvalbumin is the sole source of this Mg, a total of 82 μM [Mg] is expected to be released from parvalbumin after a single action potential.

During the rising phase of the [Ca] transient associated with a single action potential, Ca rapidly binds to divalent-cation-free Ca,Mg sites on parvalbumin (Baylor et al., 1983*a*; Maylie et al., 1987*c*). During the falling phase of the transient, Mg slowly dissociates from Mg-bound sites and is replaced by Ca from the myoplasm, a process that contributes to muscle relaxation. The amount of Ca that becomes bound to parvalbumin during this period is approximately equal to the amount of Mg that is released, 82 μM.

The amplitude of the free [Ca] transient is probably ~20 μM (Maylie et al., 1987*a*; Hirota et al., 1988) so that, according to the calculations of Maylie et al. (1987*a*, page 168; 1987*c*, Table VII), 210–220 μM [Ca] becomes bound to the Ca regulatory sites on troponin at the time of peak occupancy. During relaxation, Ca dissociates from these sites and ~82 μM, or 37–39% of the peak amount, appears to bind parvalbumin transiently (18°C).

Maylie et al. (1987*c*, pages 128 and 129) calculated the amount of Ca bound to parvalbumin from the myoplasmic [Ca] transient and the association and dissociation rate constants for Ca and Mg reacting with isolated parvalbumin. According to these calculations, 18% of the Ca that dissociates from troponin would transiently bind to parvalbumin if the myoplasmic concentration of parvalbumin were 0.5 mM. Since the calculated amount of Ca taken up by parvalbumin is directly proportional to the concentration of parvalbumin, 36% of the Ca from troponin would transiently bind if the myoplasmic concentration of parvalbumin were 1 mM, as appears to be the case in intact fibers (page 603). This value of 36% is in good agreement with the value 37–39% that is obtained from the estimated increase in myoplasmic free [Mg].

Effects of Changes in Free [Mg] on the Estimate of Free [Ca] Made with Antipyrylazo III

Since increases in free [Mg] as large as 1 mM can accompany either repetitive stimulation or voltage-clamp depolarization (Figs. 2, 5, and 7), it is important to con-

sider the effect that such increases might have on the estimates of free [Ca] made with antipyrylazo III. One effect is to increase the apparent dissociation constant of the indicator for Ca, K_D. This occurs because an increase in free [Mg] leads to an increase in the fraction of antipyrylazo III that is complexed with Mg and, consequently, a decrease in the fraction of indicator that is available to react with Ca.

K_D can be calculated on the assumption that all the antipyrylazo III inside a fiber is able to react with Ca, Mg, and other antipyrylazo III molecules in the same manner as in cuvette solutions. Under the conditions of our experiments, the total concentration of antipyrylazo III, $[Ap]_T$, would be equal to

$$[Ap]_T = [Ap] + 2[Ap_2] + [MgAp] + 2[CaAp_2]. \quad (7)$$

The terms on the right-hand side represent, from left to right, the concentrations of divalent ion-free monomers of indicator, divalent ion-free dimers, 1:1 complexes of Mg:indicator, and 1:2 complexes of Ca:indicator. K_D, the apparent dissociation constant of the 1:2 Ca:antipyrylazo III complex, is given by

$$K_D = (1 + [Mg]/K_{MgAp} + 2[Ap]/K_{D_2})^2 K_{CaAp_2}, \quad (8)$$

in which

$$K_{MgAp} = [Mg][Ap]/[MgAp], \quad (9)$$

$$K_{D_2} = [Ap][Ap]/[Ap_2], \quad (10)$$

and

$$K_{CaAp_2} = [Ca][Ap]^2/[CaAp_2]. \quad (11)$$

$K_{MgAp} = 6.7 \times 10^{-3}$ M (Rios and Schneider, 1981), $K_{D_2} = 4 \times 10^{-3}$ M (Baylor et al., 1986), and $K_{CaAp_2} = 3.51 \times 10^{-8}$ M^2 (Hollingworth et al., 1987). Baylor et al. (1986) also described cuvette calibrations that suggest the formation of 1:2 complexes of Mg:indicator at the indicator concentrations used in our experiments. Such complexes have not been included in Eqs. 7 and 8 because their dissociation constant has not been measured. If the molar extinction coefficient of $MgAp_2$ at 720 nm is similar to that of $CaAp_2$, however, the contribution of $MgAp_2$ to K_D (Eq. 8) would be negligible.

With the above values of dissociation constants, Eqs. 7–10 can be solved to give, for $[Ap]_T = 1$ mM (a typical value in our experiments), $K_D = 2.21 \times K_{CaAp_2} = 7.75 \times 10^{-8}$ M^2 for free [Mg] = 1 mM (the resting value estimated for our cut fibers, see page 587), and $K_D = 2.59 \times K_{CaAp_2} = 9.10 \times 10^{-8}$ M^2 for free [Mg] = 2 mM. Thus, in an experiment in which $[Ap]_T = 1$ mM and free [Mg] increases from 1 to 2 mM (similar to the changes we observed during either a train of action potentials or a large voltage-clamp depolarization), K_D increases by the factor 2.59/2.21 = 1.17, and any estimates of the increase in free [Ca] based on constant [Mg] = 1 mM would be too low by the factor 1.17.

The second way in which an increase in free [Mg] can affect the estimate of free Δ[Ca] is by forming 1:2 Mg:indicator complexes that absorb light at 720 nm (Baylor et al., 1986), the standard wavelength we used for measuring Ca signals. According to the cuvette calibrations of Baylor et al. (1986), an increase in free [Mg] would change $A(720)$ by an amount that is about 3×10^{-4} times as great as that produced by a similar increase in free [Ca]; the factor 3×10^{-4} should be independent of

indicator concentration since the Ca:antipyrylazo III complexes that form in the conditions of muscle fiber experiments are predominantly 1:2 (Rios and Schneider, 1981; Hollingworth et al., 1987; Maylie et al., 1987*c*). Thus, an increase in free [Mg] of 1 mM above the resting level would produce the same change in $A(720)$ as an increase in free [Ca] of ~0.3 μM above its resting level. The formation of 1:2 complexes of Mg:antipyrylazo III might contribute a significant fraction to the $\Delta A(720)$ signals observed after tetani and strong voltage-clamp depolarizations in experiments done by us (Figs. 2, 5, and 7) and by others (for example, Fig. 11 in Melzer et al., 1986).

We thank the staff of the Yale Department of Cellular and Molecular Physiology Electronics Laboratory for help with the design and construction of equipment and Dr. W. F. Boron for a sample of Me_2CF. We thank Dr. L. B. Cohen, of the Yale Department of Comparative and Mammalian Physiology, and Dr. D. W. Maughan for helpful discussion. We also thank Drs. Cohen, S. M. Baylor, M. Konishi, and P. C. Pape for providing useful comments on the manuscript.

This work was supported by the U.S. Public Health Service grants NS-07474 and AM-37643. M. Irving was initially a Science and Engineering Research Council Postdoctoral Fellow and subsequently a Royal Society University Research Fellow.

Original version received 1 August 1988 and accepted version received 27 October 1988.

REFERENCES

Baylor, S. M., W. K. Chandler, and M. W. Marshall. 1982*a*. Optical measurements of intracellular pH and magnesium in frog skeletal muscle fibres. *Journal of Physiology.* 331:105–137.

Baylor, S. M., W. K. Chandler, and M. W. Marshall, 1982*b*. Use of metallochromic dyes to measure changes in myoplasmic calcium during activity in frog skeletal muscle fibres. *Journal of Physiology.* 331:139–177.

Baylor, S. M., W. K. Chandler, and M. W. Marshall. 1983*a*. Sarcoplasmic reticulum calcium release in frog skeletal muscle fibres estimated from arsenazo III calcium transients. *Journal of Physiology.* 344:625–666.

Baylor, S. M., M. E. Quinta-Ferreira, and C. S. Hui. 1983*b*. Comparison of isotropic calcium signals from intact frog muscle fibers injected with arsenazo III or antipyrylazo III. *Biophysical Journal.* 44:107-112.

Baylor, S. M., and S. Hollingworth. 1987. Effect of calcium (Ca) buffering by fura2 on the second component of the intrinsic birefringence signal in frog isolated twitch muscle fibres. *Journal of Physiology.* 391:90P. (Abstr.)

Baylor, S. M., S. Hollingworth, C. S. Hui, and M. E. Quinta-Ferreira. 1986. Properties of the metallochromic dyes arsenazo III, antipyrylazo III and azo 1 in frog skeletal muscle fibres at rest. *Journal of Physiology.* 377:89–141.

Baylor, S. M., S. Hollingworth, and P. Pape. 1987. Myoplasmic pH transients monitored with indicator dyes in frog skeletal muscle fibers. *Biophysical Journal.* 51:549*a*. (Abstr.)

Baylor, S. M., M. E. Quinta-Ferreira, and C. S. Hui. 1985. Isotropic components of antipyrylazo III signals from frog skeletal muscle fibers. *In* Calcium in Biological Systems. R. P. Rubin, G. B. Weiss, and J. W. Putney, editors. Plenum Publishing Corp., New York. 339–349.

Chaillet, J. R., and W. F. Boron. 1985. Intracellular calibration of a pH-sensitive dye in isolated, perfused salamander proximal tubules. *Journal of General Physiology.* 86:765–794.

Endo, M., and M. Iino. 1980. Specific perforation of muscle cell membranes with preserved SR functions by saponin. *Journal of Muscle Research and Cell Motility.* 1:89-100.

Gerday, C., and J. M. Gillis. 1976. The possible role of parvalbumins in the control of contraction. *Journal of Physiology.* 258:96–97P. (Abstr.)

Godt, R. E., and D. W. Maughan. 1988. On the composition of the cytosol of relaxed skeletal muscle of the frog. *American Journal of Physiology.* 254:C591-C604.

Gosselin-Rey, C., and C. Gerday. 1977. Parvalbumins from frog skeletal muscle (*Rana temporaria L.*): isolation and characterization, structural modifications associated with calcium binding. *Biochimica et Biophysica Acta.* 492:53-63.

Gosselin-Rey, C., A. Piront, and C. Gerday. 1978. Polymorphism of parvalbumins and tissue distribution: characteristics of component I, isolated from red muscles of *Cyprinus carpio L. Biochimica et Biophysica Acta.* 532:294–304.

Haiech, J., J. Derancourt, J. F. Pechere, and J. G. Demaille. 1979. Magnesium and calcium binding to parvalbumins: evidence for differences between parvalbumins and an explanation of their relaxing function. *Biochemistry.* 18:2752–2758.

Hille, B., and D. T. Campbell. 1976. An improved Vaseline gap voltage clamp for skeletal muscle fibers. *Journal of General Physiology.* 67:265–293.

Hirota, A., W. K. Chandler, P. S. Southwick, and A. S. Waggoner. 1988. Calcium transients in frog cut twitch fibers measured with 1, 1'-dimethylmurexide-3, 3'-diacetic acid. *Biophysical Journal.* 53:647*a*. (Abstr.)

Hollingworth, S., R. W. Aldrich, and S. M. Baylor. 1987. In vitro calibration of the equilibrium reactions of the metallochromic indicator dye antipyrylazo III with calcium. *Biophysical Journal.* 51:383–393.

Hou, T., L. J. D'Anniballe, and J. A. Rall. 1988. Parvalbumin concentration in skeletal muscle fibers of the frog. *Biophysical Journal.* 53:569*a*. (Abstr.)

Irving, M., J. Maylie, N. L. Sizto, and W. K. Chandler. 1987. Passive electrical and intrinsic optical properties of cut frog twitch fibers. *Journal of General Physiology.* 89:1–40.

Johnson, J. D., D. E. Robinson, S. P. Robertson, A. Schwartz, and J. D. Potter. 1981. Ca^{++} exchange with troponin and the regulation of muscle contraction. *In* Regulation of Muscle Contraction: Excitation-Contraction Coupling. A. D. Grinnell and M. A. B. Brazier, editors. Academic Press, New York. 241–259.

Kovacs, L., E. Rios, and M. F. Schneider. 1979. Calcium transients and intramembrane charge movement in skeletal muscle fibres. *Nature.* 279:391–396.

Kovacs, L., E. Rios, and M. F. Schneider. 1983. Measurement and modification of free calcium transients in frog skeletal muscle fibres by a metallochromic indicator dye. *Journal of Physiology.* 343:161–196.

Lisman, J. E., and J. A. Strong. 1979. The initiation of excitation and light adaptation in Limulus ventral photoreceptors. *Journal of General Physiology.* 73:219–243.

Maylie, J., W. K. Chandler, M. Irving, and N. L. Sizto. 1985. Late antipyrylazo III signals in cut muscle fibers. *Biophysical Journal.* 47:351*a*. (Abstr.)

Maylie, J., M. Irving, N. L. Sizto, G. Boyarsky, and W. K. Chandler. 1987*a*. Calcium signals recorded from cut frog twitch fibers containing tetramethylmurexide. *Journal of General Physiology.* 89:145–176.

Maylie, J., M. Irving, N. L. Sizto, and W. K. Chandler. 1987*b*. Comparison of arsenazo III optical signals in intact and cut frog twitch fibers. *Journal of General Physiology.* 89:41–81.

Maylie, J., M. Irving, N. L. Sizto, and W. K. Chandler. 1987*c*. Calcium signals recorded from cut frog twitch fibers containing antipyrylazo III. *Journal of General Physiology.* 89:83–143.

Melzer, W., E. Rios, and M. F. Schneider. 1986. The removal of myoplasmic free calcium following calcium release in frog skeletal muscle. *Journal of Physiology.* 372:261–292.

Mobley, B. A., and B. R. Eisenberg. 1975. Sizes of components in frog skeletal muscle measured by methods of stereology. *Journal of General Physiology.* 66:31–45.

Ogawa, Y., and M. Tanokura. 1986. Kinetic studies of calcium binding to parvalbumins from bullfrog skeletal muscle. *Journal of Biochemistry.* 99:81–89.

O'Sullivan, W. J., and D. D. Perrin. 1964. The stability constants of metal-adenine nucleotide complexes. *Biochemistry.* 3:18–26.

Potter, J. D., J. D. Johnson, J. R. Dedman, W. E. Schreiber, F. Mandel, R. L. Jackson, and A. R. Means. 1977. Calcium binding proteins: relationship of binding, structure, conformation and biological function. *In* Calcium-binding Proteins and Calcium Function. R. H. Wasserman, R. A. Corradino, E. Carofoli, and R. H. Kretsinger, editors. North-Holland, Amsterdam. 239–250.

Quinta-Ferreira, M. E., S. M. Baylor, and C. S. Hui. 1984. Antipyrylazo III (Ap III) and Arsenazo III (Az III) calcium transients from frog skeletal muscle fibers simultaneously injected with both dyes. *Biophysical Journal.* 45:47*a*. (Abstr.)

Rios, E., and M. F. Schneider. 1981. Stoichiometry of the reactions of calcium with the metallochromic indicator dyes Antipyrylazo III and Arsenazo III. *Biophysical Journal.* 36:607–621.

Smith, R. M., and A. E. Martell. 1976. Critical Stability Constants. Vol. 4: Inorganic Complexes. Plenum Publishing Corp., New York. p. 56.

Somlyo, A. V., H. Gonzalez-Serratos, H. Shuman, G. McClellan, and A. P. Somlyo. 1981. Calcium release and ionic changes in the sarcoplasmic reticulum of tetanized muscle: an electron probe study. *Journal of Cell Biology.* 90:577–594.

Suarez-Kurtz, G., and I. Parker. 1977. Birefringence signals and calcium transients in skeletal muscle. *Nature.* 270:746–748.